

# Plasmodium Sporozoite Motility Is Modulated by the Turnover of Discrete Adhesion Sites

Sylvia Münter,<sup>1,6</sup> Benedikt Sabass,<sup>2,6</sup> Christine Selhuber-Unkel,<sup>4,6</sup> Mikhail Kudryashev,<sup>1</sup> Stephan Hegge,<sup>1</sup> Ulrike Engel,<sup>3</sup> Joachim P. Spatz,<sup>4</sup> Kai Matuschewski,<sup>1</sup> Ulrich S. Schwarz,<sup>2,5,\*</sup> and Friedrich Frischknecht<sup>1,\*</sup>

<sup>1</sup>Parasitology, Department of Infectious Diseases, University of Heidelberg Medical School, Im Neuenheimer Feld 324

<sup>2</sup>Bioquant, Im Neuenheimer Feld 267

<sup>3</sup>Bioquant, Nikon Imaging Center, Im Neuenheimer Feld 267

University of Heidelberg, 69120 Heidelberg, Germany

<sup>4</sup>Max Planck Institute for Metals Research, Department of New Materials and Biosystems and University of Heidelberg,

Department of Biophysical Chemistry, Heisenbergstr. 3, 70569 Stuttgart, Germany

<sup>5</sup>Institute of Zoology, Theoretical Biophysics Group, University of Karlsruhe, Kaiserstrasse 12, 76131 Karlsruhe, Germany

<sup>6</sup>These authors contributed equally to this work

\*Correspondence: [ulrich.schwarz@bioquant.uni-heidelberg.de](mailto:ulrich.schwarz@bioquant.uni-heidelberg.de) (U.S.S.), [freddy.frischknecht@med.uni-heidelberg.de](mailto:freddy.frischknecht@med.uni-heidelberg.de) (F.F.)

DOI 10.1016/j.chom.2009.11.007

## SUMMARY

Sporozoites are the highly motile stages of the malaria parasite injected into the host's skin during a mosquito bite. In order to navigate inside of the host, sporozoites rely on actin-dependent gliding motility. Although the major components of the gliding machinery are known, the spatiotemporal dynamics of the proteins and the underlying mechanism powering forward locomotion remain unclear. Here, we show that sporozoite motility is characterized by a continuous sequence of stick-and-slip phases. Reflection interference contrast and traction force microscopy identified the repeated turnover of discrete adhesion sites as the underlying mechanism of this substrate-dependent type of motility. Transient forces correlated with the formation and rupture of distinct substrate contact sites and were dependent on actin dynamics. Further, we show that the essential sporozoite surface protein TRAP is critical for the regulated formation and rupture of adhesion sites but is dispensable for retrograde capping.

## INTRODUCTION

Cell migration is a complex and highly regulated process that plays a crucial role in a large range of physiological and disease-related situations. Eukaryotic cell motility is dependent on the concerted action of actin and myosin and is often initiated by actin-driven extensions of the forward (leading) membrane, followed by the establishment of new contact sites to the substrate and the release of contacts at the rear end. Quantitative microscopy studies of migrating mammalian cells have revealed many details about the role of actin and myosin and its relation to the continuous formation and turnover of integrin-mediated adhesion sites (Vicente-Manzanares et al., 2009; Wang, 2007). In contrast, little is known about these

processes of protozoa, including the medically important apicomplexan parasites that feature motile invasive stages such as *Plasmodium* or *Toxoplasma* (Heintzelman, 2006). These parasites constitute highly polarized and simple-shaped cells that show limited types of motile behavior (Frixione et al., 1996; Vanderberg, 1974). Their main mode of active locomotion is actomyosin-dependent gliding motility that is important for migration across tissue barriers and host cell invasion (Heintzelman, 2006).

The main components that constitute the core of the gliding machinery are known (Daher and Soldati-Favre, 2009; Frénel and Soldati-Favre, 2009; Schüler and Matuschewski, 2006), but the spatiotemporal dynamics of the individual proteins inside the complex and, hence, the underlying mechanism that powers forward locomotion still remain unclear. Studies on malaria parasites and the related apicomplexan parasite *Toxoplasma gondii* revealed that the myosin motor proteins are anchored into an alveolate-specific membrane system, the inner membrane complex (IMC), and that short actin filaments might be linked to plasma membrane proteins (Baum et al., 2008; Daher and Soldati-Favre, 2009). The motility machinery of malaria parasites is important for the merozoite and ookinete stages to invade red blood cells of the host and traverse the midgut epithelium of the mosquito vector, respectively (Cowman and Crabb, 2006; Vlachou et al., 2006). A third invasive stage, the *Plasmodium* sporozoite, forms in oocysts at the mosquito midgut wall, is released into the hemolymph, and penetrates the salivary glands (Matuschewski, 2006). Sporozoites isolated from the salivary glands of an infected mosquito move on solid substrates along circular paths, without changing their shape, at an average speed of 1–2  $\mu\text{m/s}$  (Vanderberg, 1974). Within the cavities and ducts of salivary glands, only few sporozoites move at low velocities (Frischknecht et al., 2004). However, once injected into the skin of a host, sporozoites move on seemingly random paths at similar speeds as in vitro and eventually invade blood or lymph vessels (Amino et al., 2006). Sporozoites that entered the blood can furthermore move on the endothelium of blood vessels and invade hepatocytes, where they differentiate into thousands of red blood cell-infecting merozoites (Frevert et al., 2005). The mechanisms underlying gliding motility are

therefore essential for the progression through the malaria lifecycle.

In marked contrast to higher eukaryotic cells, actin filaments of *Plasmodium* parasites are elusive *in vivo*. Until now, no actin filaments could be revealed in living or fixed malaria parasites, and purified parasite actin only polymerizes into filaments of less than 100 nm length *in vitro* (Sahoo et al., 2006; Schmitz et al., 2005; Schüler et al., 2005). A high turnover of short actin filaments in *Plasmodium* parasites might be necessary to achieve the high speed of sporozoites. The actin filaments of the sporozoite are thought to be linked via the glycolytic F-actin-binding enzyme aldolase to the substrate by the thrombospondin-related anonymous protein (TRAP) (Baum et al., 2008; Morahan et al., 2009). TRAP, like its orthologs in other apicomplexan parasites and malaria parasite stages, is stored in specific organelles at the apical (front) tip of the parasites and secreted during cell motility (Morahan et al., 2009). In analogy to actin-based motility of higher eukaryotic cells, it was predicted that sporozoites establish contacts to the substratum over which the actomyosin motor pushes the parasite forward (Baum et al., 2008; Ménard, 2001). Eventually, TRAP is cleaved by specialized proteases at the posterior (rear) end of the parasites and is released into the membrane and protein-rich trail left behind moving parasites (Baker et al., 2006; Dowse et al., 2008). Thus, the sequence of secretion, adhesion formation, and cleavage is thought to lead to continuous gliding.

Here, we used reflection interference contrast microscopy (RICM) and traction force microscopy (TFM) to show that sporozoite motility is limited by the dynamic turnover of discrete adhesion sites, which leads to a stick-and-slip movement of the cell.

## RESULTS

### Motility and Adhesion Pattern of Sporozoites *In Vivo* and *In Vitro*

*In vivo* imaging at low frame rates (0.5 Hz) has revealed that sporozoites move irregularly within tissues (Amino et al., 2006; Frischknecht et al., 2004). To resolve parasite motility at higher temporal resolution, we first imaged sporozoites in salivary canals, in the skin, and on cultured hepatocytes at 2 Hz (Figure 1A). Speed plots revealed that sporozoites move in a stop-and-go fashion, with periods of rapid movement followed by periods of slow movement. This irregularity observed *in vivo* and on cultured cells could be caused by both internal and external factors. We therefore imaged sporozoite gliding on glass surfaces and found similar motion patterns (Figure 1B), suggesting that internal processes contribute to the irregular trajectories. No difference in the overall speed was found between sporozoites moving on glass, on cells or in the skin (Figure 1C and see also [Experimental Procedures](#)). Quantification of the tracks from parasites gliding inside of the different tissues and *in vitro* revealed that, during periods of rapid movement, sporozoites traveled up to one parasite length (Figure 1D).

In order to investigate whether, as in mammalian cells, discrete adhesion sites are formed and possibly modulate motility, we employed reflection interference contrast microscopy (RICM) (Rädler and Sackmann, 1992; Sengupta et al., 2006) (Figure S1A available online). For the initial stage of

adhesion, RICM clearly showed that the sporozoite first adheres with one end, then with the second end, and finally with the cell body (Figure S1B). Importantly, RICM revealed a nonuniform distribution of adhesion sites on the surface of the parasite, as defined by dark areas along the cell (Figures 2A and S1C–S1E and [Movie S1](#)). The absolute intensity level of the reflected light differed from one sporozoite to the other, with parasites showing larger adhesion zones moving at a slower speed (Figure 2B and [Movie S1](#)). Analysis of more than 100 motile sporozoites showed that, usually, a small adhesion site was present at the front and one or two adhesion sites at the rear of the sporozoite (Figures 2A and 2C).

### Adhesion Turnover Rate Correlates with Overall Sporozoite Speed

The occurrence of discrete sites of adhesion and their dynamics during motility suggest that parasite motility might function differently than previously anticipated (Baum et al., 2008; Ménard, 2001). RICM revealed the turnover of discrete adhesion sites to be linked to changes in gliding speed, showing a thrust when the rear end of the parasite detached from the substrate. Moreover, the formation of a new adhesion site was found to slow down motility (Figures 2C, 2D, and S2). As slowly moving sporozoites showed fewer changes in their adhesion patterns, they underwent fewer cycles of speed changes per time (Figures 2E and S3). Examination of the dynamics of readily distinguishable adhesion sites at the front and rear of 22 independent sporozoites showed a linear correlation between adhesion site turnover and speed (Figure 2F), confirming that speed is strongly determined by adhesion. Importantly, the frequency of speed peaks (periods of fast movement; see [Figure S4](#)) correlated with the frequency of observed adhesion cycles (Figure 2F). Speed peaks could be defined and automatically detected (Figure S4). This enabled an alternative calculation of the runlength during a speed peak, which essentially yielded the same result as the wavelet analysis: sporozoites typically travel less than their own length during one period of fast movement (Figures 1D and S4F). We also noted that sporozoites usually did not change their overall average speed over time (Figures S3D and S3E). Even those sporozoites that interrupted their motility for some time usually continued gliding at the same speed as before. All examined sporozoites moved in a stop-and-go fashion, and even slow-moving ones relied on adhesion turnover for short periods of rapid movement.

We next mapped the crescent shapes of the sporozoites onto linear ones, which allowed us to measure temporal changes in the intensity distribution of the reflected light along the central axis of the cell body. The resulting kymographs revealed that the adhesion sites at the very front and rear moved along with the parasite during locomotion. In contrast, the larger adhesion sites in the central part show more complex dynamics, with a mixed pattern of staying fixed with the parasite and undergoing retrograde movement (Figure 3). Our data suggest that parasite motility can be described in a first approximation as an alternating sequence of periods of run and firm adhesion. Most importantly, resting time dominates the average velocity, suggesting a functional relevance of the observed stick-slip frequencies ([Supplemental Text](#)).

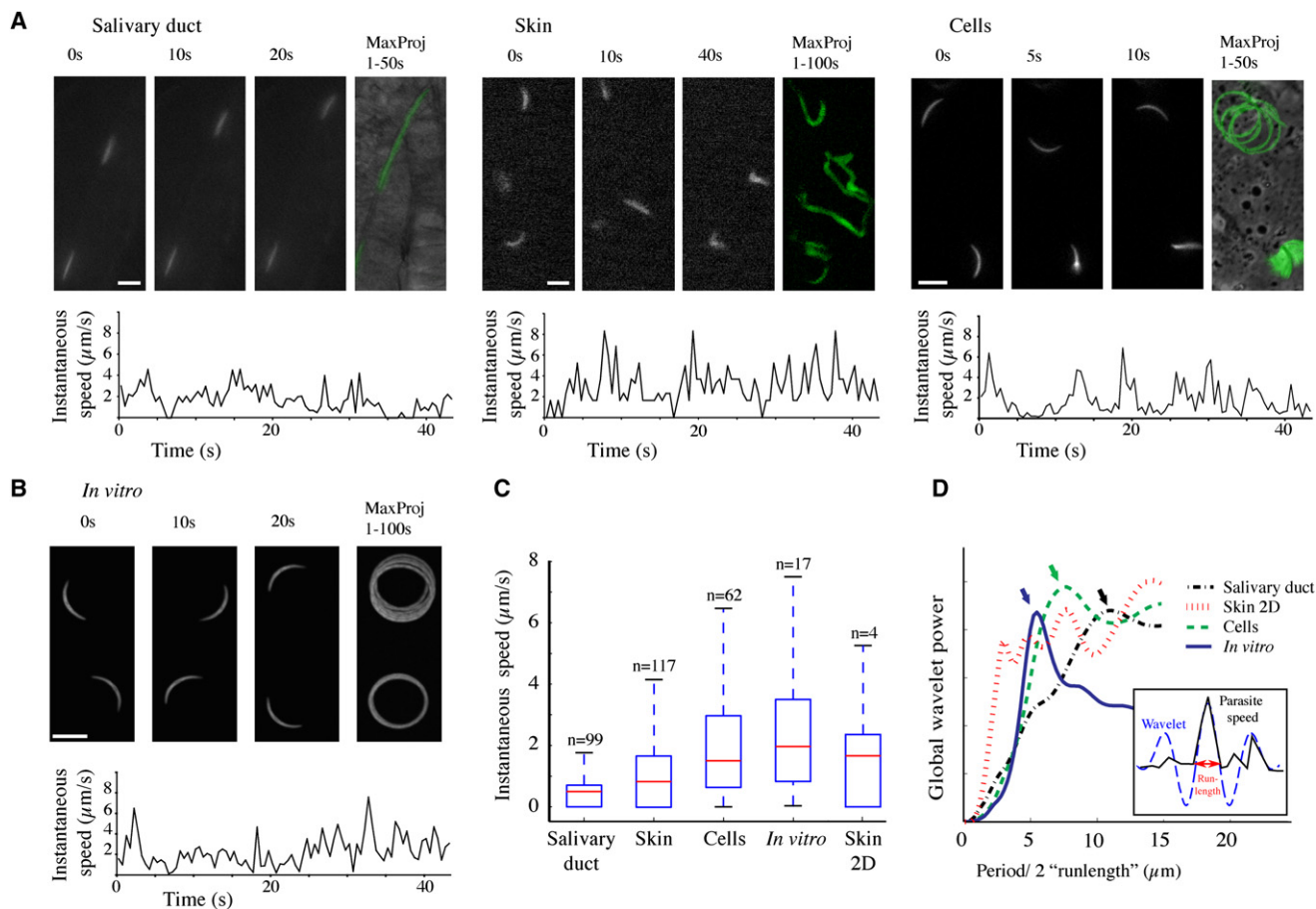


**Figure 1. Motility Pattern of Sporozoites In Vivo and In Vitro**

(A) Speed plot and fluorescence images of sporozoites tracked inside of the salivary duct, inside of the skin, and on cultured hepatocytes. Three consecutive fluorescence images and the maximum projection of the fluorescence intensity from an entire time-lapse sequence (green) are shown; for salivary duct and liver cells, the transmission image was overlaid. Numbers indicate time in seconds. Scale bars, 10  $\mu\text{m}$ .

(B) Speed plots and fluorescence images of sporozoites tracked on glass cover slides. Scale bar, 10  $\mu\text{m}$ .

(C) Plot of instantaneous speeds from parasites gliding in the different environments. Boxes contain 50% of data distributed around its median (red bar). Whiskers show the range of data. Sporozoites in the skin, which migrate within one focal plane, are labeled with "Skin 2D." This distinction is necessary to avoid tracking errors (see [Experimental Procedures](#)). Numbers above the bars indicate the number of tracked sporozoites. For each sporozoite, the instantaneous speed was determined at 2 Hz over 50 to 300 frames.

(D) Global wavelet power spectrum (see [Experimental Procedures](#)) showing a peak (arrows) at the typical length that sporozoites move during one speed peak ("runlength"). Intuitively, this method can be pictured as fitting half of a period of a sine into each speed peak and thus finding the average width of the peaks (small inset). Abscissa: half of the center period of the wavelets. Ordinate: global power spectrum normalized to maximum.

### Traction Force Applied by the Parasites on the Substrate

Our observations of the adhesive dynamics suggest that sporozoites generate variable forces at discrete adhesion sites. To test this prediction, we used traction force microscopy (TFM) on soft elastic substrates with embedded marker beads ([Dembo and Wang, 1999](#); [Sabass et al., 2008](#)) (Figures 4A, S5A, and S5B and [Movie S2](#)). Image processing and computational reconstruction of the cellular traction pattern of sporozoites showed that, during continuous gliding, the central part of the parasite exerted forces perpendicular to its direction of movement (Figures 4A and 4B and [Movies S3 and S4](#)). Strikingly, forces pointing along the direction of movement were preferentially localized at both ends, where the long-lived adhesions were observed in RICM (Figure 2A). Statistical analysis of six gliding sporozoites shows that forces in the center are larger than forces

produced at the front or rear (Figure 4C). These data suggest that one has to distinguish between perpendicular forces along the cell body and longitudinal forces at the ends (Figure 4D, left). Forces perpendicular to the cell axis could be partially due to nonspecific adhesion between the elastic substrate and the sporozoite, as predicted by contact mechanics of elastic bodies ([Johnson, 1985](#)) (Figure 4D, right).

Intriguingly, analysis of ten independent parasites showed that strong forces at the rear were invariably linked to time frames during which sporozoites became immobilized with their rear but continued to pull forward with their front, therefore stretching the parasite (Figures 4E and 4F). These apparent stalling forces pointed into the direction of movement. At the front of the parasite, similar forces are transmitted independently of the forward speed of the parasite (Figure 4F). In contrast, the forces

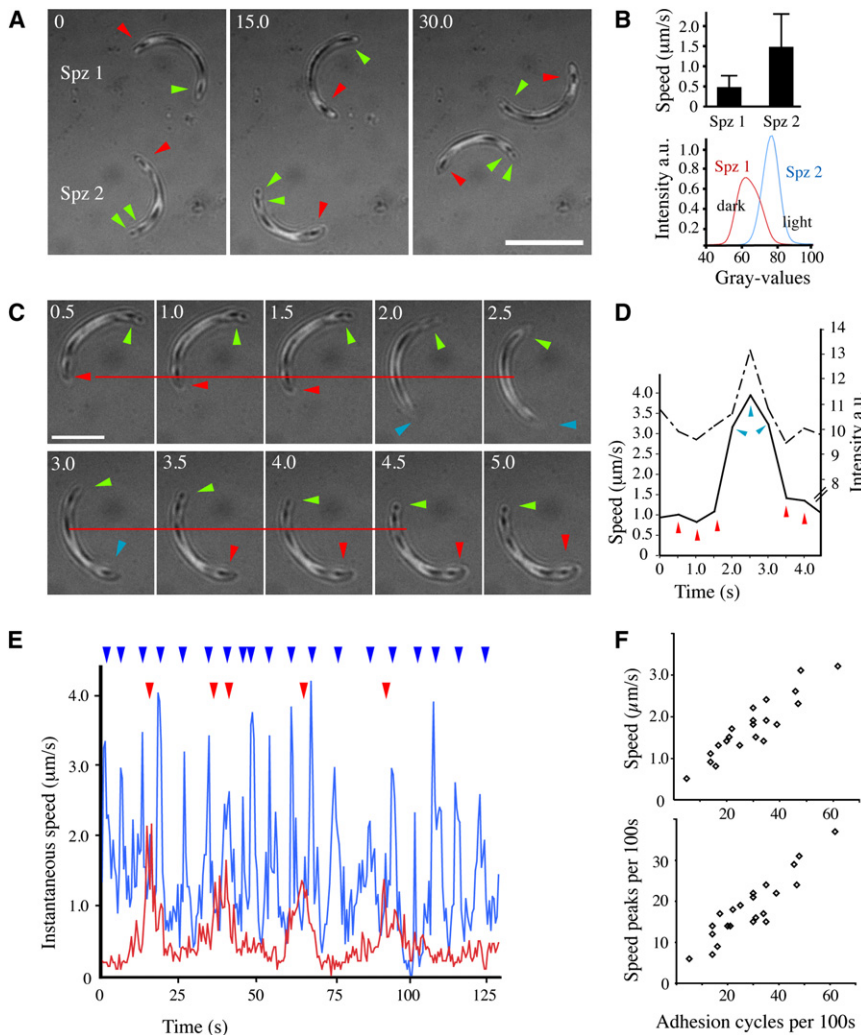


**Figure 2. Turnover of Discrete Adhesion Sites Results in Irregular Sporozoite Motility**

(A) Time-lapse RICM images of one slow (Spz1) and one fast (Spz2) gliding sporozoite. Most adhesion sites stay fixed (arrowheads) in respect to the moving sporozoite. Numbers indicate time in seconds. Scale bar, 10  $\mu\text{m}$ . See also [Movie S1](#). (B) Analysis of the sporozoites in (A). The slow-moving Spz1 (speed plot; top) has larger adhesions (darker average RICM intensities; bottom).

(C) A sporozoite accelerates upon disassembly of adhesion sites at the front and rear. Red line indicates tip of the sporozoite in the first frame.

(D) Speed plot from the frames shown in (C). High speed correlates with lighter areas in RICM, reflecting less adhesion.

(E) The instantaneous speed plotted against time of the two parasites shown in (A) (Spz1 in red; Spz2 in blue). Arrowheads indicate speed peaks.

(F) The frequency of adhesion cycles at front or rear is proportional to the average speed as well as to the frequency of speed peaks of gliding parasites ( $R^2 = 0.84$  and  $0.77$ , respectively). Twenty-two sporozoites were examined for 100–200 frames each.

transmitted by the same parasite at the center and rear ends were larger during slower movement (sticking), supporting the hypothesis that the adhesion sites at the rear end slow down movement (Figure 4F).

### Correlation of Force Measurements with Adhesion Site Turnover

The incompatibility of a combined RICM and TFM analysis precludes direct comparisons of adhesion site dynamics with local forces. However, the movement of the parasites on glass and the flexible substrate is highly similar, and some parasites do repeatedly get immobilized at the rear end during the continuous circular motility on both substrates. Therefore, we could readily find sticking parasites using RICM ([Movie S5](#)). Similarly to parasites moving on glass or elastic gels, these parasites changed their curvature from  $0.24 \mu\text{m}^{-1}$  to  $0.17 \mu\text{m}^{-1}$  during stretching, while their length stayed constant. Analysis of stretching parasites by RICM revealed that, during stretching, the parasites built a new adhesion site at their center (Figure 4G). During sticking, the front of the parasite moved faster than the rear, and only after release of the rear, its speed surpassed

briefly the speed of the front (Figure 4H). Interestingly, the main traction force during stretching originated not at the adhesion site at the front end, but was distributed to the adhesion site toward the center of the sporozoite, indicating a flattening of the parasite (Figures 4E and 4F). Every stretching event went along with a subsequent thrust in speed, suggesting that the presence of the rearward adhesion is the main restriction for movement (Figures 4H and S5C and [Movie S5](#)).

Measuring the front-to-rear distance of a parasite and analyzing the speed peaks together with the intensity of the rear-end adhesion, as well as the stretching of the parasite, showed that these three parameters are highly coordinated. Decrease in adhesion, which is revealed as an increase in pixel intensity, strongly correlates with an increase in speed (Figures 5A and 5B). Quantitative analysis confirmed that weakening of the adhesion at the rear end positively correlates with the speed, and in accordance to this, the stretching shows a negative correlation with the speed of the parasites (Figure 5C). Accordingly, the traveled path of the rear end is shorter after a sticking period of the parasite (Figure 5D). Therefore, the TFM data together with RICM showed that sporozoite motility results from active force generation transmitted through distinct adhesion sites.

### Influence of Actin-Interfering Drugs on Parasite Motility

The irregular motion patterns most likely result from the interplay of the force-generating (actomyosin) and -transmitting (surface adhesion receptors) machinery. We therefore investigated sporozoites gliding on glass under a range of concentrations of jasplakinolide (Jas), which inhibits actin depolymerization, and cytochalasin D (CytoD), which inhibits actin polymerization

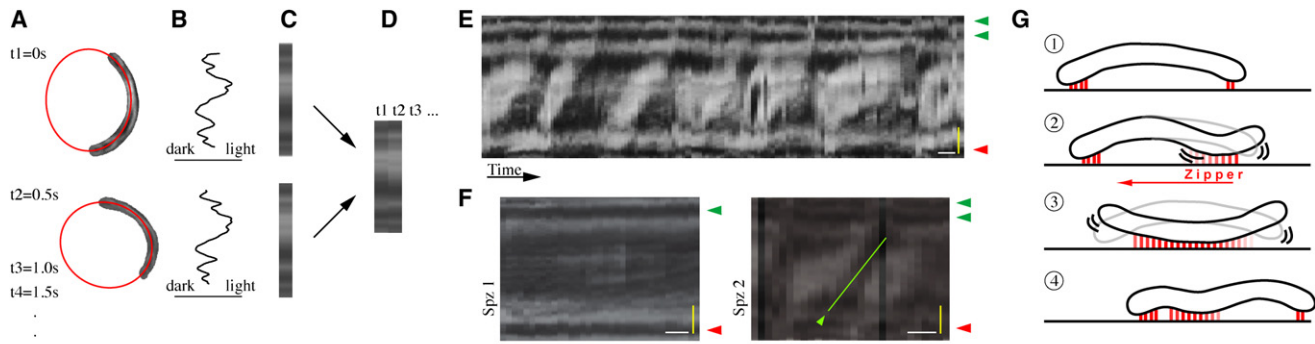


**Figure 3. Generation of Kymographs from Gliding Sporozoites**

(A) The central axis of the parasite was defined by fitting an ellipse.

(B) The intensity profile of the parasite along the ellipse (radial average: 6 pixels) was extracted.

(C) The intensities along the ellipse were visualized by expanding the intensity profile to a rectangle.

(D) The kymograph was generated by stringing together a series of rectangular profiles obtained from (C) for subsequent images ( $t_1, t_2, \dots$ ).

(E) Kymograph of a fast gliding sporozoite (average speed:  $1.8 \mu\text{m/s}$ ) for 70 s. The front and rear adhesions (red and green arrowheads, respectively) stay fixed with respect to the moving parasite. In the center of the cell body, a more complex scenario is observed, with mixed patterns of stable adhesions and their retrograde motion. Scale bars, 2 s (white) and  $2.5 \mu\text{m}$  (yellow).

(F and G) (F, left) Kymograph of the slow-moving sporozoite (Spz 1 from Figure 2A) showing only some irregularities in the central adhesions. Again, front and rear adhesions (red and green arrowheads, respectively) stay fixed with respect to the moving parasite.

(F, right) Kymograph of the fast-moving sporozoite (Spz 2 from Figure 2A). The light-green arrowhead indicates an adhesive region moving rearward at a higher speed than the sporozoite forward movement. Scale bars, 2 s (white) and  $2.5 \mu\text{m}$  (yellow).

(G) Cartoon showing that the faster rearward movement can be explained by a zipper-like adhesion seemingly moving at higher inverse speed than the parasite as the respective parts of the sporozoite approach the substrate.

(Cooper, 1987; Cramer, 1999). Average and maximum speeds were highest at low concentrations of Jas. Both speeds decreased with increasing concentrations for Jas and CytoD (Figures 6A and S6A). Parasites gliding on elastic substrates under 50 nM CytoD that moved with half of the average speed of controls showed traction forces of about half of control forces (Figures 6B and 6C). Curiously, parasites moving at the same average speed as control sporozoites but under 100 nM Jas showed forces of only about a quarter of those from controls (Figures 6B and 6C). Imaging sporozoites moving at 25% of control speed in 100 nM CytoD with RICM showed an increased adhesion turnover rate. In contrast, sporozoites moving at 50% of control speed under 200 nM Jas showed a lower rate of adhesion turnover, with the front and rear ends staying longer in contact with the substrate (Figures 6D and S6B and Movies S6 and S7). This indicates that increased F-actin weakens adhesion strengths and turnover. As expected, at high concentrations of both inhibitors, sporozoites stopped moving, and turnover of adhesion sites dropped dramatically (Figure 6E). However, when a sudden hydrodynamic flow was applied to sporozoites, they remained better attached under high concentrations of CytoD than in the absence of drugs, and they readily detached under high concentrations of Jas (Figures 6F and S7), confirming that more F-actin leads to weaker adhesion.

### The Role of TRAP on the Adhesion Turnover during Gliding Motility

Sporozoite adhesion is mediated through different surface proteins, including TRAP. Moreover, it has been shown that TRAP forms a link between the extracellular substrate and the actin cytoskeleton (Morahan et al., 2009). *trap(-)* sporozoites still form inside of the mosquito midgut and circulate in the hemolymph but can no longer enter the salivary glands (Sultan

et al., 1997). In order to investigate the role of TRAP in sporozoite locomotion, we imaged *trap(-)* and wild-type (WT) sporozoites isolated from the mosquito hemolymph. As expected, most attached wild-type parasites were gliding in circles, and the majority of attached *trap(-)* sporozoites were not moving. However, *trap(-)* parasites were still able to build adhesion sites (Figure 7A). In addition, both *trap(-)* and WT parasites from the hemolymph showed a new type of motility that we termed patch gliding (Figures 7B and S8). A similar type of motility, termed pendulum gliding, has been described earlier for parasites expressing only a truncated or mutated cytoplasmic tail of TRAP (Kappe et al., 1999). According to this report, mutant parasites appear to glide fully attached for one body length, followed by an arrest for 1–2 s and backward movement along the same axis. In marked contrast, patch gliding sporozoites from the hemolymph of WT or *trap(-)* parasites do not stop, can move at speeds exceeding those of circular gliding sporozoites, and describe noncircular trajectories. Using RICM and fast DIC imaging, we found that patch gliding sporozoites continuously move over a single spot in a back-and-forth manner at similar speeds in both directions (Movie S8). We also observed *trap(-)* parasites that were attached to the substrate at one end to translocate particles in both anterograde and retrograde direction with indistinguishable speeds (Figure 7C). Both particle movements and patch gliding were abolished with CytoD (Movie S9). *trap(-)* sporozoites could undergo patch gliding for extended periods of time (several minutes) without completing adhesion. However, once they formed a second adhesion, *trap(-)* sporozoites were no longer able to rupture this contact site (Movie S10). Comparing the behavior of WT with *trap(-)* parasites confirmed that *trap(-)* parasites were not capable of exhibiting normal gliding motility (Sultan et al., 1997), and the percentage of floating and waving parasites was higher

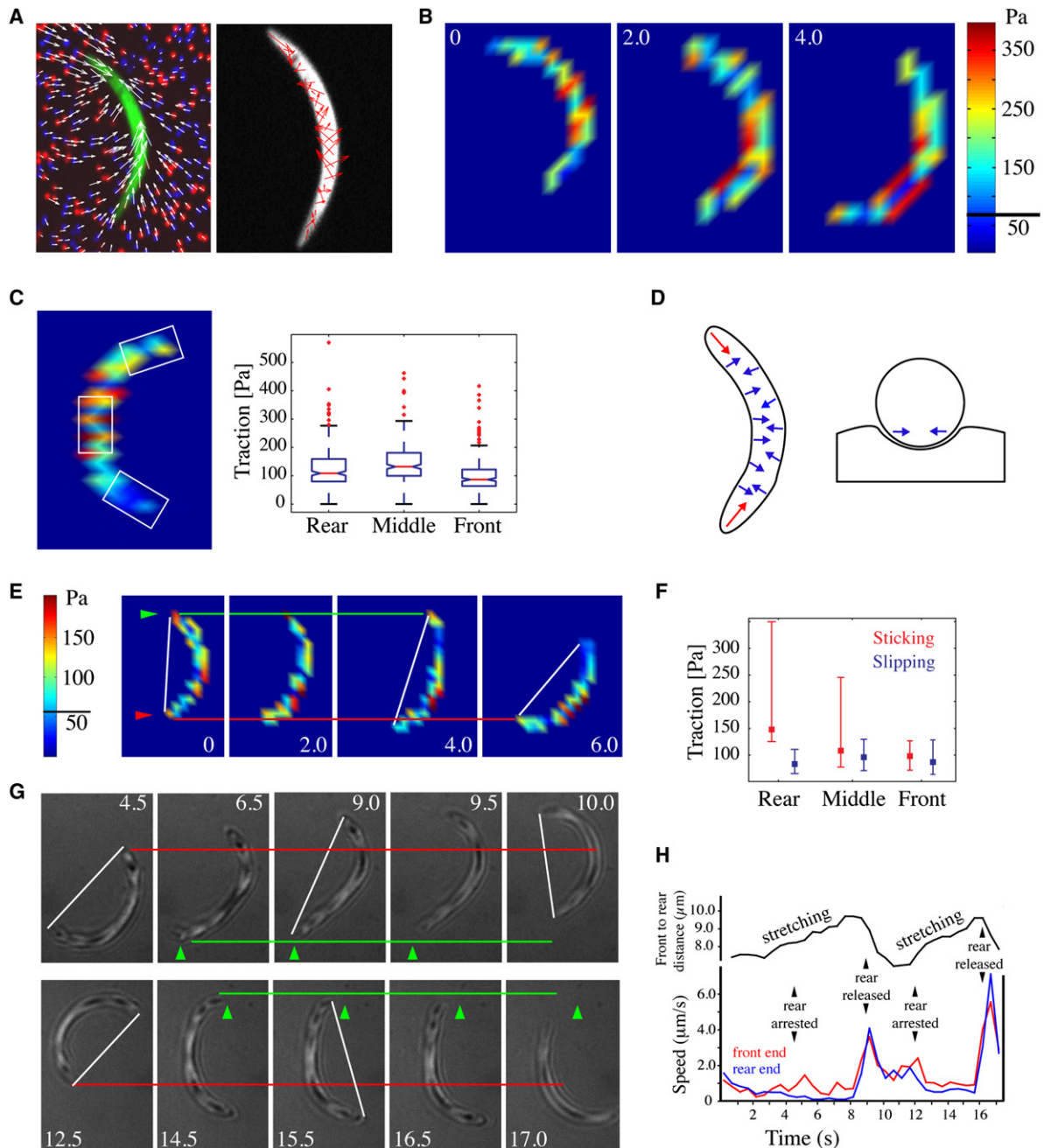


**Figure 4. Traction Forces Correlate with Adhesion Dynamics during Sporozoite Gliding**

(A) (Left) Sporozoite on a flexible polyacrylamide gel containing fluorescent red and far-red (pseudocolored in blue) marker beads. The arrows show bead displacements. (Right) Traction vectors (red) are reconstructed from displacement data. See also *Movies S2–S4*.

(B) Pseudocolored traction force maps (Pa, Pascal). Numbers indicate time in seconds. Bar in force scale indicates noise ( $2\sigma$ ). See also *Movie S3*.

(C) Comparing forces at the front end, the central region, and the rear end of six gliding sporozoites (each from about 50 frames). Nonoverlapping notches indicate that distributions differ at a significance level below 5%, as also determined by a Kruskal-Wallis test.

(D) Cartoon showing the directionality of traction (force vectors) in gliding sporozoites. Central forces might result mainly from contact adhesion.

(E) Strong forces are detected at the rear and at the center during sporozoite stretching. The white line indicates the front (red arrowhead) to rear (green arrowhead) distance (Pa, Pascal).

(F) Bootstrap analysis of the force distribution of ten parasites during slipping and stretching. During sticking, large forces appear at the rear. Bar corresponds to 95% confidence of Bootstrap analysis.

(G) Adhesion dynamics and speed changes during sporozoite stretching as visualized with RICM. A sporozoite getting stuck twice at the rear (green arrowheads and green line) stretches before releasing the rear and regaining its crescent shape. The white line indicates the front-to-rear distance. See also *Movie S5*.

(H) The graph shows that stretching increases until release of the rear leads to a speed peak.

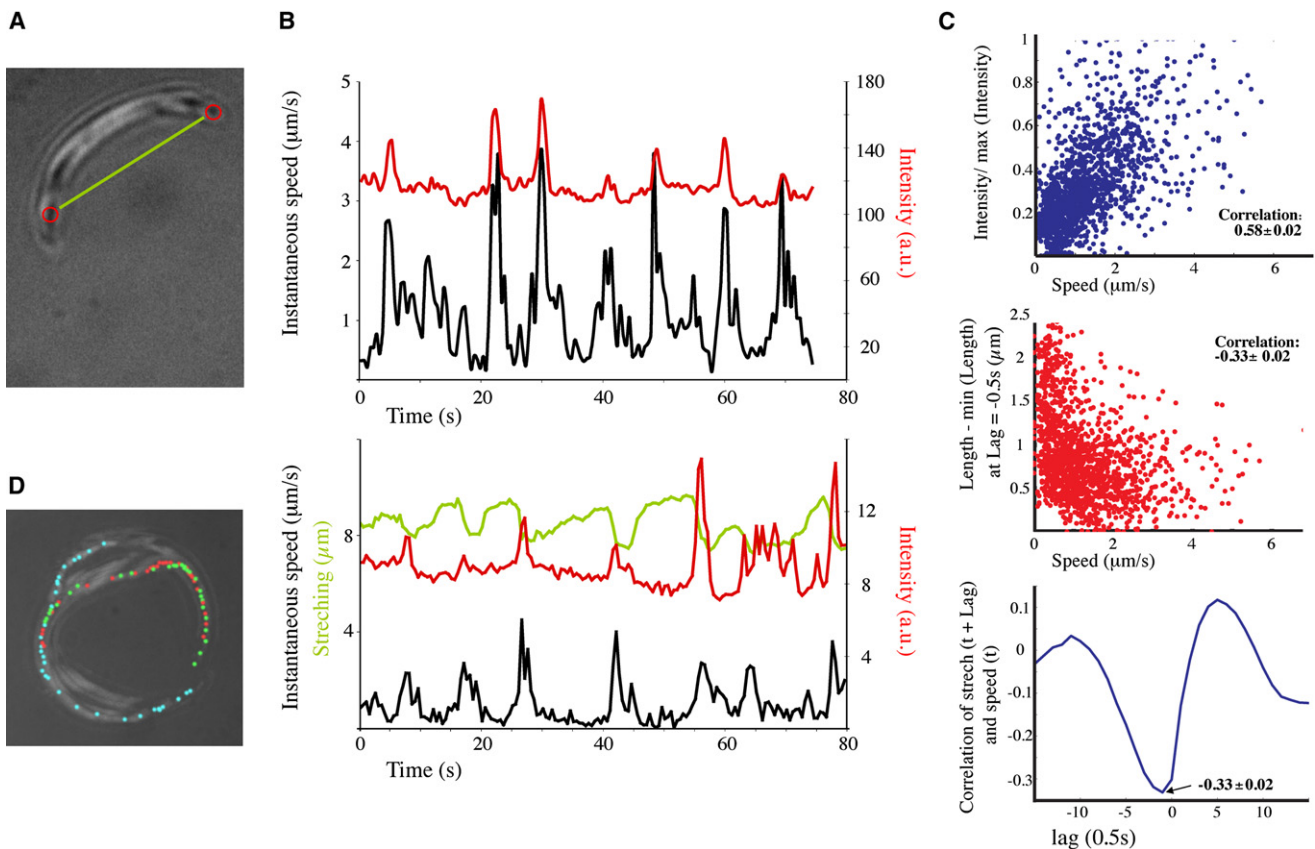


**Figure 5. Correlation of Speed with Attachment and Stretching of the Parasites**

(A) RICM image of a sporozoite. The two red circles indicate the spots on which the parasites were manually tracked at the front and rear ends. The green line indicates the distance calculated from the tracking coordinates of the front and rear. For the intensity analysis, the pixels located in a radius of 7 pixels around the  $x/y$  coordinates of the tracked points were summed.

(B) Top graph shows the speed of the sporozoite rear end (black curve) and the intensity measured for the rear adhesion spot (red curve). The bottom graph shows stretching of a different parasite (green curve) in addition to the speed and the intensity of the spot at the rear. Note the almost perfect correlation of stretching with the increase in speed and distance from the substrate.

(C) Quantitative analysis and correlation of the events highlighted in (B) from seven parasites (about 200 time frames each). (Top) Positive correlation of the intensity of the rear-end adhesion (defined in A) with the average speed. (Middle) Negative correlation of the stretching with the average speed of the parasites. (Bottom) The maximum stretch of a parasite is regularly followed by a speed peak. Correlation between stretch and speed displays a clear minimum for a lag of 0.5 s, showing that the speed peak occurs during the shortening rather than after it. Standard deviations of correlations were calculated with the Bootstrap method.

(D) For a parasite stuck with the rear end, the traveled path of the rear end (the two adhesion dots at the rear end of the parasites are tracked in red and green, respectively) after rupture is shorter than the traveled path of the front end (light blue dots).

compared to WT parasites (Figure 7D). These observations show that TRAP is important, but not essential, for initial parasite adhesion. They also show that TRAP is important in detachment of sporozoite adhesion sites, suggesting that TRAP plays a major role in coordinating continuous gliding motility through the turnover of contact sites. Most importantly, TRAP appears to be dispensable for slipping. In contrast to the role of TRAP, actin seems to have a role in both adhesion turnover and slipping (Figure 7E).

## DISCUSSION

### Stick-Slip Motility of Sporozoites

Here, we show that *Plasmodium* sporozoites move in a stick-slip manner that is regulated by the formation and turnover of distinct adhesion sites. Our *in vitro* approach enabled us to use surface-

sensitive microscopy techniques to investigate the role of the adhesion dynamics for gliding motility of malaria parasites. RICM revealed distinct adhesion sites during initial sporozoite adhesion and motility. Surprisingly, the sporozoite did not translocate over the initial adhesion site at the front, as postulated previously (Baum et al., 2008; Ménard, 2001). Instead, sporozoites could move at slow speed without changing front and rear adhesion patterns in respect to the moving parasite (Figure 2A). Slow-moving sporozoites could speed up by disengaging the front or rear adhesion sites. Strikingly, the frequency of these events correlated with the overall average speed of the parasites (Figures 2E and 2F). It thus appears that, in addition to classic gliding, i.e., backward capping of adhesion proteins, sporozoites also use adhesion turnover at the front and rear ends to regulate their speed. Using traction force microscopy, we found a large stalling force at the rear adhesion sites,

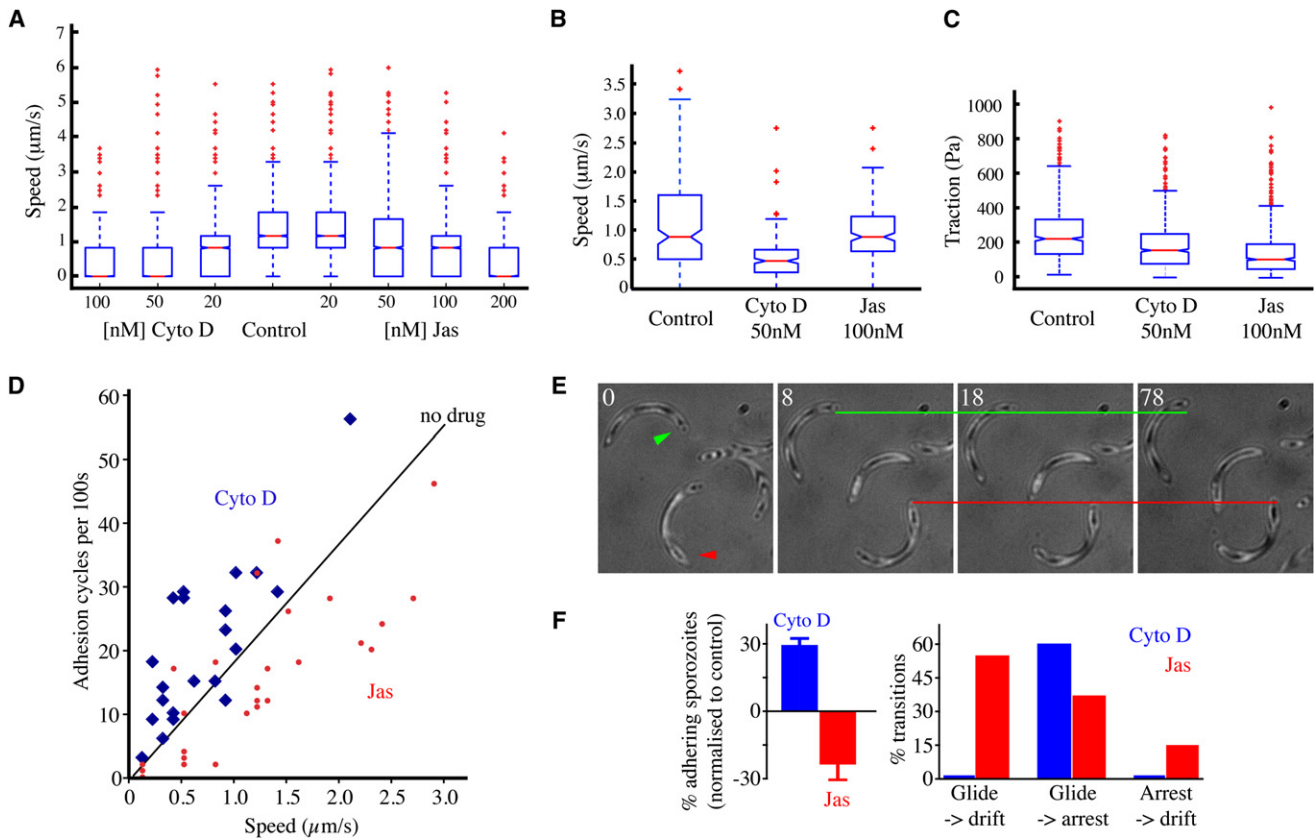


**Figure 6. Actin-Disrupting Drugs Modulate Traction Force and Adhesion Turnover**

(A) Parasite speed on glass at different concentrations of CytoD and Jas ( $n > 10$  in each condition). In both cases, speed decreases at sufficiently high drug concentrations.

(B) Speed of selected parasites gliding on the elastic substrate under control and drug conditions.

(C) Traction forces generated by the sporozoites shown in (B) decrease for both drug treatments. Parasites under Jas show even lower forces despite unaltered speed.

(D) For each speed value, the frequency of adhesion cycles increases for 100 nM CytoD (blue diamonds) and decreases for 200 nM Jas (red circles), respectively. Linear fit (black line) shows the control parasites (Figure 2F). See also Movies S6 and S7.

(E) Gliding sporozoites exposed to high concentrations of CytoD show extended arrest and enhanced adhesion lifetimes. Red and green arrow and line indicate front and rear, respectively, of the parasites. Numbers indicate time in seconds.

(F) Effect of a disrupting shear flow. (Left graph) Under shear, the percentage of adherent sporozoites increases and decreases if treated with CytoD and Jas, respectively. (Right graph) Sporozoite motion under shear can be classified as gliding in circles, drifting with the flow, or arrest. Under shear, the dominant transition for CytoD is “gliding arrest”, whereas for Jas, considerably more transitions to drift occur, indicating that adhesion strength is weakened.

especially right before rupture of this adhesion. The adhesion site on the front exerted much less force. Large forces also appeared in the center of the parasite, but the irregular motion pattern in this region makes it difficult to correlate force generation with the appearance of adhesion sites (Figure 4). Furthermore, the forces at the center of the parasite were directed perpendicularly to the direction of movement. It is likely that the central forces are mainly nonproductive adhesion forces that are important in keeping the parasite in contact with the substrate. The rapid changes in the force and speed patterns after rupture of adhesion sites suggests that elastic energy is built up during sticking and then released during slipping, similar to stick-slip phenomena in the sliding friction of nonbiological material.

#### TRAP and Actin Dynamics Modulate Adhesion Turnover

Apart from these mechanical insights, we also identified new roles for actin and TRAP during gliding. Investigation of mutant

sporozoites lacking *TRAP* as well as WT sporozoites in the presence of actin dynamic-inhibiting molecules revealed a number of unexpected findings. Most importantly, *TRAP* is not essential for the translocation of the parasite over an adhesion site because mutant parasites still perform a fast and actin-dependant, albeit nondirectional, slipping motility that we termed patch gliding (Figure 7). Instead, *TRAP* appears to play an essential role in initial parasite adhesion and a major role in coordinating regular gliding motility through deadhesion of contact sites. As there are two TRAP-like proteins present in *Plasmodium* sporozoites, TLP and S6 (also named TREP) (Combe et al., 2009; Heiss et al., 2008; Moreira et al., 2008; Steinbuechel and Matuschewski, 2009), an interesting question is how these proteins contribute to both adhesion modulation and gliding. This issue could be addressed in the future by the generation of double knockout parasites and domain-swap experiments. It will be further of interest whether these proteins are colocalized on the sporozoite

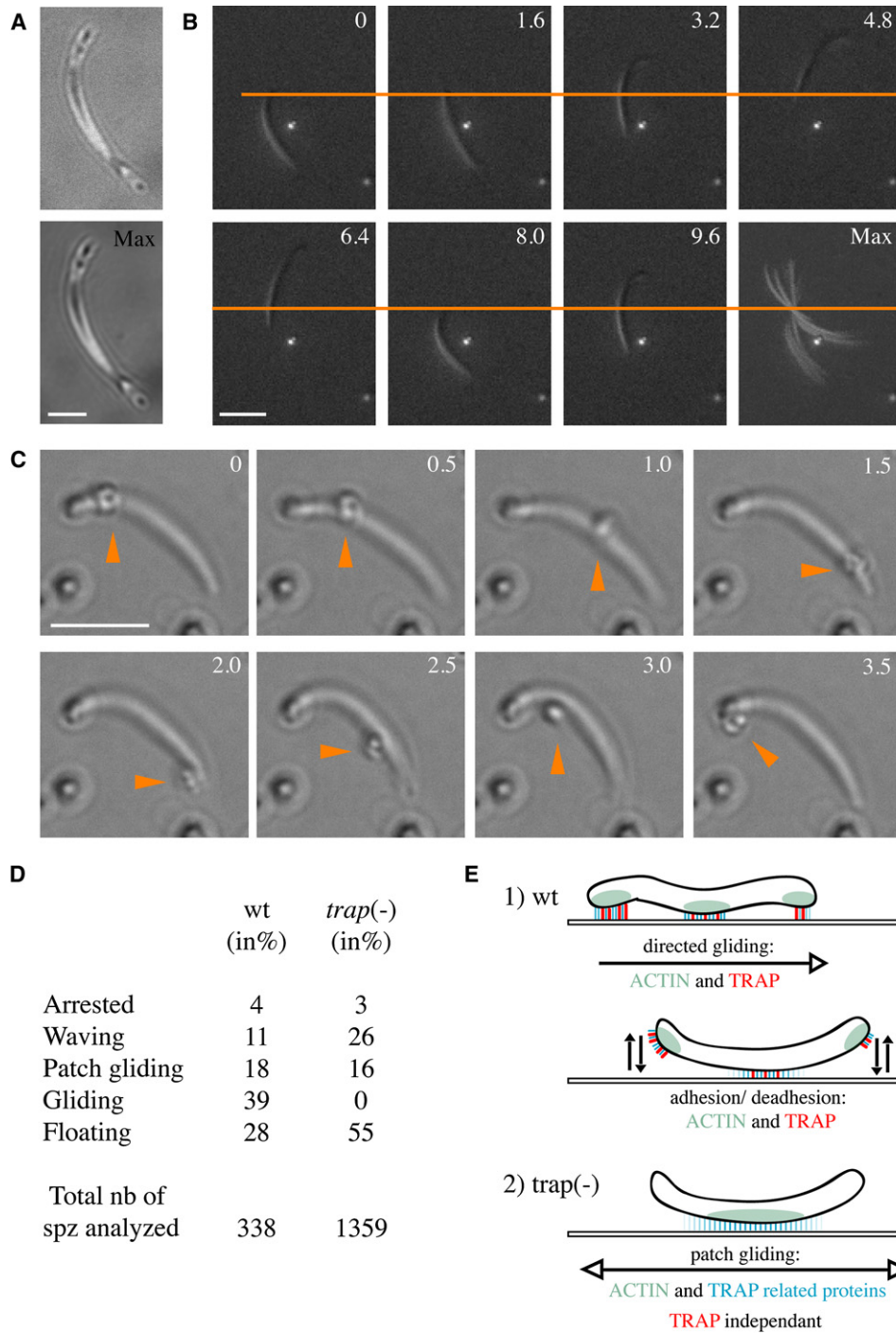


**Figure 7. *trap(-)* Mutants Are Deficient in Deadhesion**

(A) *trap(-)* mutants can build the same adhesion sites compared to WT parasites (one at the front and two at the rear); however, they are not able to glide once the discrete adhesions at the front and rear are formed. A single frame (top) and the maximum projection (Max) of a movie of 110 s.

(B) Sporozoites from the hemolymph, including the *trap(-)* mutant shown here, often display patch gliding during which the cell moves forth and back over a single adhesion site (orange line). See also [Movie S8](#).

(C) A particle (orange arrowhead) is observed to be translocated in both directions over the *trap(-)* sporozoite surface in a way reminiscent of patch gliding. See also [Movie S9](#).

(D) Classification and quantification of hemolymph sporozoite motility patterns into arrested, waving, patch gliding, gliding in circles, and floating free in solution.

(E) Model illustrating that *TRAP* plays a role in adhesion formation and turnover (deadhesion), whereas actin plays a dual role in adhesion dynamics and slipping. *TRAP* is dispensable for rapid patch gliding (slipping) and might regulate a switch, which converts adhesion dynamics into directed motion. Arrows indicate direction of slipping. Molecules are marked with matching colors.

surface. Interestingly, TRAP appears not to be uniformly distributed on the cell surface (Gantt et al., 2000; Kappe et al., 1999). How this distribution relates to our findings, however, is unclear. Furthermore, it will be interesting to investigate how the TRAP-cleaving rhomboid protease (Baker et al., 2006; Dowse et al., 2008) modulates adhesion turnover. Actin dynamics appeared to play a dual role during sporozoite motility. Surprisingly we found that increased levels of F-actin, induced by the addition of increasing concentrations of Jas, led to less adhesion dynamics, weaker adhesion forces, and, eventually, detachment of the sporozoite (Figures 6 and S7). This finding suggests that elevated F-actin leads to less traction at the same speed. As the forces decrease with increasing speed in the absence of drugs (Figure 4F), it appears that fast-moving sporozoites contain more F-actin. Similarly, it was shown for *T. gondii* tachyzoites that these parasites move faster under small concentrations of Jas (Wetzel et al., 2003). In contrast, the actin filament-disrupting drug CytoD led to increased adhesion dynamics. Curiously, despite reduced traction forces in the presence of CytoD, more sporozoites stay attached at high concentrations of the drug under flow conditions (Figure 6F). Therefore, traction force seems to peak at an intermediate concentration of F-actin. We thus postulate that actin filaments are not just required for retrograde movement of the plasma membrane proteins, but also for establishment and turnover of discrete adhesion sites at the front and rear of the parasites (Figures 6D and 7E). A direct demonstration of actin filaments using electron microscopy would clearly be helpful but has not yet been achieved for intact sporozoites (M.K., unpublished data; Lepper et al., 2010).

In conclusion, we suggest that actin filaments together with TRAP likely regulate the turnover of discrete parasite adhesion sites. More F-actin could lead to weaker adhesion and less adhesion dynamics. During motility, TRAP possibly coordinates the formation of contact sites and the dissociation of these contact sites from the substrate. The observed interplay of force generation and adhesion is reminiscent of the way that mammalian cells link the actomyosin system with integrins to achieve cell adhesion. It also raises the possibility that a parasite myosin, as well as a set of signaling proteins, participate in sporozoite adhesion dynamics.

## EXPERIMENTAL PROCEDURES

### Preparation and Imaging of Sporozoites

*Plasmodium berghei* (strain NK65) sporozoites expressing the green fluorescent protein (GFP) and *trap(-)* parasites (Sultan et al., 1997) were produced in *Anopheles stephensi* mosquitoes and sporozoites harvested essentially as described in Frischknecht et al. (2004) and Hegge et al. (2009).

Imaging inside of the salivary duct was performed as described (Frischknecht et al., 2004) with 3% bovine serum albumin. For imaging on cells, Huh7 cells (cultivated in RPMI supplemented with 10% fetal calf serum) were transferred on a glass bottom Petri dish 1 day prior to the experiment, and the sporozoites were added in RPMI 3% BSA. The parasites were filmed on the Huh7 cells as well as in between the cells on the glass surface, at 37°C. The latter parasites served as controls for this experiment (Figure 1). All image acquisitions were performed on an inverted Axiovert 200M Zeiss microscope using a GFP filter set. Images were collected with a Zeiss AxioCam HRm at 2 Hz using Axiovision 4.6 software and a 25× LCI Plan-Neofluar objective (NA 0.8). In vivo imaging was essentially performed as described in Amino et al. (2006) using the PerkinElmer UltraView spinning disc confocal unit on an inverted

Nikon TE 2000-E microscope through a 20× objective (PlanFluor multi-immersion NA 0.75) but at a 2 Hz imaging rate.

For drug treatment, isolated sporozoites were placed in a 96-well glass bottom plate (Corning, Germany), and the drugs (CytoD and Jas) were added in the indicated concentrations. Imaging was performed at 2–16 Hz also on the PerkinElmer spinning disc confocal with a 20× (Nikon PlanFluor multi-immersion NA 0.75) or 100× (Nikon Plan Apo VC NA 1.4) objective. Speed plots represent either average speed over several tens of seconds or “instantaneous speed” when at least one image was recorded per second and the speed from one to the next frame was plotted. For limitations of accurate speed measurements, see Hegge et al. (2009).

For flow measurements, sporozoites were placed in an uncoated flow chamber (Ibidi, Germany) and imaged on an inverted Axiovert 200M using a GFP filterset at room temperature. Images were collected at 1 Hz using a 10× Apoplan objective (NA 0.25). For the perfusion of drugs, a 100 μM stock solution in PBS was used and mixed inside the flow chamber during continuous image acquisition. Unidirectional flow was applied by adding 2 ml of medium to one buffer container of the flow chamber.

RICM is a surface-sensitive optical technique that has been frequently used for studying the adhesion of vesicles and cells (Sengupta et al., 2006) (Figure S1A). RICM was set up on an inverted Axiovert 200 Zeiss microscope with a Antiflex Plan-Neofluar 63× objective (NA 1.25) using the 546.1 nm line of a mercury lamp (HBO 103, Osram, Germany). Images of sporozoites in glass bottom dishes were recorded at 2 Hz with a CCD camera (ORCA-ER, Hamamatsu, Japan) using simplePCI software (Hamamatsu, Japan).

All image series were eventually imported to ImageJ for analysis, and figures were generated using the Adobe Creative Suite software package. Pixel sizes were preserved during image processing.

### Wavelet-Based Runlength Measurement

The global wavelet power spectrum quantifies, analogous to a usual power spectrum, the scale dependence of a function's behavior. However, the wavelet transform uses local basis functions, thus providing information about frequency and time. Here, we used a Morlet ( $\sigma = 5$ ) wave function. The tracked sporozoite movement was parameterized as  $v(x)$  [speed(path)], and the width of the speed peaks is then the desired runlength. A wavelet analysis was conducted on the concatenated data of all sporozoites. Multiple permutations of the sequences served to suppress any possible effect due to the concatenation of endpoints of individual sequences. The global wavelet power spectrum is the average  $\langle F(s,x)F^*(s,x) \rangle_x$ , in which  $s$  is the scale of the wavelet,  $x$  is the sporozoite path, and  $F$  is the wavelet transformed data. A scale corresponding to the average width of the speed peaks contributes a peak to the wavelet power spectrum. One advantage of using wavelet analysis instead of regular Fourier analysis lies in the fact that the wavelet power spectrum is usually smoother than is the frequency spectrum. More importantly, we also found that the irregular duration of slow periods between the speed peaks does not affect the wavelet analysis as strongly as it does for the Fourier analysis.

### Parasite Tracking

Sporozoites were either manually tracked at the apical end (RICM) using the manual tracking plug-in of ImageJ, semiautomatically tracked using the MTrack2 plug-in for ImageJ, or analyzed with a recently developed software based on MTrack2 that is part of Fiji ([http://pacific.mpi-cbg.de/wiki/index.php/Main\\_Page](http://pacific.mpi-cbg.de/wiki/index.php/Main_Page)) (Hegge et al., 2009). Adhesion cycles were counted manually on RICM acquisitions and normalized to the number of cycles occurring during 100 s. One adhesion cycle was defined as follows: parasite front or rear touching the surface (i.e., a dark spot) until either of both is released (dark spot disappeared) and reattached (dark spot reappeared).

For tracking of in vivo movement, z projections were performed prior to tracking. This results in the loss of the speed vector in z direction and thus an underestimation of average speed. It also provides a potential pitfall for speed detection of movement in the direction of the light path (z direction). We therefore identified parasites that moved only within a single optical plane and tracked and analyzed those. This showed an increase of speed compared to the combined data from all sporozoites moving in the skin (Figures 1A–1C).

### Speed Peak and Runlength Detection

Speed peak detection was performed on time series from manually (RICM) and automatically tracked parasites imaged at 1–4 Hz. A speed peak was defined if the following conditions were fulfilled: (1) the instantaneous speed was larger than the median value of the entire sequence of the tracked parasite; (2) the instantaneous speed was highest compared to the three time points before and after; (3) the instantaneous speed surpasses 150% of the minimal value from three or seven time points before and after the actual position (the two different window sizes were used to detect both very sharp and rather wide peaks); and (4) two adjacent peaks could not be closer than 2 s. For comparison between tracks, the frequency of peak occurrence was calculated for every track as number of speed peaks detected divided by the total duration of the track.

In order to test the stability of the peak determination routine, we added extra conditions as: a speed peak should be over a global threshold  $k_c$  – an absolute value determining the minimum value of the speed peak.

The runlength of a parasite during a speed peak was calculated as a sum of the instantaneous speeds around a speed peak (three values before and after the speed peak) and the two adjacent values on each side (radius of five time points around one speed peak). This value was multiplied by the lapsed time to get the runlength in  $\mu\text{m}$ .

### Traction Force Microscopy

Elastic gel substrates were prepared as described before (Wang and Pelham, 1998). We mixed two different marker beads: either 0.1  $\mu\text{m}$  yellow-green and 0.2  $\mu\text{m}$  red fluorescent beads or 0.2  $\mu\text{m}$  red and 0.2  $\mu\text{m}$  dark-red fluorescent beads (Invitrogen, Germany). The relative concentrations of acrylamide and bisacrylamide were chosen according to Yeung et al. (2005) to permit the usage of published values for the elastic moduli. The parasites were placed directly onto the gel and were covered with a 22  $\times$  22 mm glass coverslip. Image acquisition was performed on the Nikon-PerkinElmer spinning disc confocal with a 100 $\times$  objective (Nikon Plan Apo VC NA 1.4). Images were collected with an EM-CDD camera (Orca ER Hamamatsu, Japan) at 1 Hz using the UltraView software (PerkinElmer).

Traction forces were reconstructed as described previously (Sabass et al., 2008). Displacements of red and green (red and far-red, respectively) fluorescent marker beads embedded in the polyacrylamide gel reflect the effect of traction applied by the sporozoite to the surface of the gel. We thus compared images of sporozoites adhering at different sites in the field of view to find the relative substrate displacements. A Poisson ratio around 0.5 justified the assumption that the effect of vertical “pulling” of the sporozoite was decoupled from the lateral traction; hence, we interpreted all bead displacements as a sole result of lateral traction. We used either a boundary element method or Fourier transform traction cytometry to determine the traction at the nodes of our prescribed mesh. In the case of the Fourier Transform method, we implemented an iterative procedure similar to the one described in Butler et al. (2002) to include the information about the cell contour. Here, we found it necessary to use zero-patterning techniques to avoid traction artifacts at the outer rim of the cell.

### Statistical Analysis

Significant differences in the traction force or speed data were displayed visually with the help of the notched whisker plots using groups of data through five-number summaries: the sample minimum, the lower and upper quartiles, the median, and the sample maximum. Maxima and minima are defined as the extreme data points within a range of 2 times the distance between upper and lower quartile, centered on the average of the quartiles. Outliers, marked as red points, are those data points that are beyond the above range. Nonoverlapping notches are used to indicate significant differences between medians. The notch displays the 95% confidence interval for the median based on the assumption of a normal distribution. Significant differences were validated with a nonparametric Kruskal-Wallis test.

### SUPPLEMENTAL DATA

Supplemental Data include Supplemental Text, eight figures, and ten movies and can be found with this article online at [http://www.cell.com/cell-host-microbe/supplemental/S1931-3128\(09\)00384-9](http://www.cell.com/cell-host-microbe/supplemental/S1931-3128(09)00384-9).

### ACKNOWLEDGMENTS

We thank R. Richter for help with RICM; A. Besser, M. Cyrklaff, M. Ganter, G. Gerisch, S. Lepper, and M. Meissner for discussions and/or reading of the manuscript; D. Scheppan for mosquito infection; and the Nikon Imaging Center at the University of Heidelberg for access to their microscopes. This work was supported by grants from the German Federal Ministry for Education and Research (BMBF-BioFuture) to F.F.; the German Research Foundation (DFG, SFB 544) to F.F.; and the Frontier Program of the University of Heidelberg to U.S.S. and F.F. This work was supported, in part, by the Institute for Computational Modeling; Siberian Branch of the Russian Academy of Science, Krasnoyarsk; the Center for Modelling and Simulation (BIOMS); and the Cluster of Excellence CellNetworks and the Medical School at the University of Heidelberg. The Max Planck Society and the Karlsruhe Institute of Technology (KIT) and its Concept for the Future are acknowledged. K.M. and F.F. are members of the European Network of Excellence BioMalPar.

Received: August 11, 2009

Revised: October 21, 2009

Accepted: November 19, 2009

Published: December 16, 2009

### REFERENCES

- Amino, R., Thiberge, S., Martin, B., Celli, S., Shorte, S., Frischknecht, F., and Ménard, R. (2006). Quantitative imaging of Plasmodium transmission from mosquito to mammal. *Nat. Med.* 12, 220–224.
- Baker, R.P., Wijetila, R., and Urban, S. (2006). Two Plasmodium rhomboid proteases preferentially cleave different adhesins implicated in all invasive stages of malaria. *PLoS Pathog.* 2, e113.
- Baum, J., Gilberger, T.W., Frischknecht, F., and Meissner, M. (2008). Host-cell invasion by malaria parasites: insights from Plasmodium and Toxoplasma. *Trends Parasitol.* 24, 557–563.
- Butler, J.P., Tolić-Nørrellykke, I.M., Fabry, B., and Fredberg, J.J. (2002). Traction fields, moments, and strain energy that cells exert on their surroundings. *Am. J. Physiol. Cell Physiol.* 282, C595–C605.
- Combe, A., Moreira, C., Ackerman, S., Thiberge, S., Templeton, T.J., and Ménard, R. (2009). TREP, a novel protein necessary for gliding motility of the malaria sporozoite. *Int. J. Parasitol.* 39, 489–496.
- Cooper, J.A. (1987). Effects of cytochalasin and phalloidin on actin. *J. Cell Biol.* 105, 1473–1478.
- Cowman, A.F., and Crabb, B.S. (2006). Invasion of red blood cells by malaria parasites. *Cell* 124, 755–766.
- Cramer, L.P. (1999). Role of actin-filament disassembly in lamellipodium protrusion in motile cells revealed using the drug jasplakinolide. *Curr. Biol.* 9, 1095–1105.
- Daher, W., and Soldati-Favre, D. (2009). Mechanisms controlling glideosome function in apicomplexans. *Curr. Opin. Microbiol.* 12, 408–414.
- Dembo, M., and Wang, Y.L. (1999). Stresses at the cell-to-substrate interface during locomotion of fibroblasts. *Biophys. J.* 76, 2307–2316.
- Dowse, T.J., Koussis, K., Blackman, M.J., and Soldati-Favre, D. (2008). Roles of proteases during invasion and egress by Plasmodium and Toxoplasma. *Subcell. Biochem.* 47, 121–139.
- Frénal, K., and Soldati-Favre, D. (2009). Role of the parasite and host cytoskeleton in apicomplexa parasitism. *Cell Host Microbe* 5, 602–611.
- Frevert, U., Engelmann, S., Zougbedé, S., Stange, J., Ng, B., Matuschewski, K., Liebes, L., and Yee, H. (2005). Intravital observation of Plasmodium berghei sporozoite infection of the liver. *PLoS Biol.* 3, e192.
- Frischknecht, F., Baldacci, P., Martin, B., Zimmer, C., Thiberge, S., Olivio-Marin, J.C., Shorte, S.L., and Ménard, R. (2004). Imaging movement of malaria parasites during transmission by Anopheles mosquitoes. *Cell. Microbiol.* 6, 687–694.
- Frixione, E., Mondragón, R., and Meza, I. (1996). Kinematic analysis of Toxoplasma gondii motility. *Cell Motil. Cytoskeleton* 34, 152–163.

- Gantt, S., Persson, C., Rose, K., Birkett, A.J., Abagyan, R., and Nussenzweig, V. (2000). Antibodies against thrombospondin-related anonymous protein do not inhibit *Plasmodium* sporozoite infectivity in vivo. *Infect. Immun.* **68**, 3667–3673.
- Hegge, S., Kudryashev, M., Smith, A., and Frischknecht, F. (2009). Automated classification of *Plasmodium* sporozoite movement patterns reveals a shift towards productive motility during salivary gland infection. *Biotechnol. J.* **4**, 903–913.
- Heintzelman, M.B. (2006). Cellular and molecular mechanics of gliding locomotion in eukaryotes. *Int. Rev. Cytol.* **251**, 79–129.
- Heiss, K., Nie, H., Kumar, S., Daly, T.M., Bergman, L.W., and Matuschewski, K. (2008). Functional characterization of a redundant *Plasmodium* TRAP family invasin, TRAP-like protein, by aldolase binding and a genetic complementation test. *Eukaryot. Cell* **7**, 1062–1070.
- Johnson, K.L. (1985). *Contact mechanics* (Cambridge: Cambridge University Press).
- Kappe, S., Bruderer, T., Gantt, S., Fujioka, H., Nussenzweig, V., and Ménard, R. (1999). Conservation of a gliding motility and cell invasion machinery in Apicomplexan parasites. *J. Cell Biol.* **147**, 937–944.
- Lepper, S., Merkel, M., Sartori, A., Cyrklaff, M., and Frischknecht, F. (2010). Rapid quantification of the effects of blotting for correlation of light and cryo-light microscopy. *J. Microsc.* Published online October 22, 2009. 10.1111/j.1365-2818.2009.03327.x.
- Matuschewski, K. (2006). Getting infectious: formation and maturation of *Plasmodium* sporozoites in the *Anopheles* vector. *Cell. Microbiol.* **8**, 1547–1556.
- Ménard, R. (2001). Gliding motility and cell invasion by Apicomplexa: insights from the *Plasmodium* sporozoite. *Cell. Microbiol.* **3**, 63–73.
- Morahan, B.J., Wang, L., and Coppel, R.L. (2009). No TRAP, no invasion. *Trends Parasitol.* **25**, 77–84.
- Moreira, C.K., Templeton, T.J., Lavazec, C., Hayward, R.E., Hobbs, C.V., Kroeze, H., Janse, C.J., Waters, A.P., Sinnis, P., and Coppi, A. (2008). The *Plasmodium* TRAP/MIC2 family member, TRAP-Like Protein (TLP), is involved in tissue traversal by sporozoites. *Cell. Microbiol.* **10**, 1505–1516.
- Rädler, J., and Sackmann, E. (1992). On the measurement of weak repulsive and frictional colloidal forces by reflection interference contrast microscopy. *Langmuir* **8**, 848–853.
- Sabass, B., Gardel, M.L., Waterman, C.M., and Schwarz, U.S. (2008). High resolution traction force microscopy based on experimental and computational advances. *Biophys. J.* **94**, 207–220.
- Sahoo, N., Beatty, W., Heuser, J., Sept, D., and Sibley, L.D. (2006). Unusual kinetic and structural properties control rapid assembly and turnover of actin in the parasite *Toxoplasma gondii*. *Mol. Biol. Cell* **17**, 895–906.
- Schmitz, S., Grainger, M., Howell, S., Calder, L.J., Gaeb, M., Pinder, J.C., Holder, A.A., and Veigel, C. (2005). Malaria parasite actin filaments are very short. *J. Mol. Biol.* **349**, 113–125.
- Schüler, H., and Matuschewski, K. (2006). Regulation of apicomplexan microfilament dynamics by a minimal set of actin-binding proteins. *Traffic* **7**, 1433–1439.
- Schüler, H., Mueller, A.K., and Matuschewski, K. (2005). Unusual properties of *Plasmodium falciparum* actin: new insights into microfilament dynamics of apicomplexan parasites. *FEBS Lett.* **579**, 655–660.
- Sengupta, K., Aranda-Espinoza, H., Smith, L., Janmey, P., and Hammer, D. (2006). Spreading of neutrophils: from activation to migration. *Biophys. J.* **91**, 4638–4648.
- Steinbuechel, M., and Matuschewski, K. (2009). Role for the *Plasmodium* sporozoite-specific transmembrane protein S6 in parasite motility and efficient malaria transmission. *Cell. Microbiol.* **11**, 279–288.
- Sultan, A.A., Thathy, V., Frevert, U., Robson, K.J., Crisanti, A., Nussenzweig, V., Nussenzweig, R.S., and Ménard, R. (1997). TRAP is necessary for gliding motility and infectivity of *Plasmodium* sporozoites. *Cell* **90**, 511–522.
- Vanderberg, J.P. (1974). Studies on the motility of *Plasmodium* sporozoites. *J. Protozool.* **21**, 527–537.
- Vicente-Manzanares, M., Choi, C.K., and Horwitz, A.R. (2009). Integrins in cell migration—the actin connection. *J. Cell Sci.* **122**, 199–206.
- Vlachou, D., Schlegelmilch, T., Runn, E., Mendes, A., and Kafatos, F.C. (2006). The developmental migration of *Plasmodium* in mosquitoes. *Curr. Opin. Genet. Dev.* **16**, 384–391.
- Wang, Y.L. (2007). Flux at focal adhesions: slippage clutch, mechanical gauge, or signal depot. *Sci. STKE* **2007**, pe10.
- Wang, Y.L., and Pelham, R.J., Jr. (1998). Preparation of a flexible, porous polyacrylamide substrate for mechanical studies of cultured cells. *Methods Enzymol.* **298**, 489–496.
- Wetzal, D.M., Håkansson, S., Hu, K., Roos, D., and Sibley, L.D. (2003). Actin filament polymerization regulates gliding motility by apicomplexan parasites. *Mol. Biol. Cell* **14**, 396–406.
- Yeung, T., Georges, P.C., Flanagan, L.A., Marg, B., Ortiz, M., Funaki, M., Zahir, N., Ming, W., Weaver, V., and Janmey, P.A. (2005). Effects of substrate stiffness on cell morphology, cytoskeletal structure, and adhesion. *Cell Motil. Cytoskeleton* **60**, 24–34.